

Article

Experimental and Modelling Study of Pt, Pd, and 2E+Au Flotation Kinetics for Platreef Ore by Exploring the Influence of Reagent Dosage Variations

Parisa Doubra *, Candice Carelse, Deshenthree Chetty and Marian Manuel

Mintek, 200 Malibongwe Drive, Randburg, Johannesburg 2194, South Africa; candicec@mintek.co.za (C.C.); deshch@mintek.co.za (D.C.); marianm@mintek.co.za (M.M.)

* Correspondence: parisad@mintek.co.za; Tel.: +27-(11)-709-4032

Abstract: This study investigates the flotation kinetics of individual platinum-group elements (PGEs) and gold, namely Pt, Pd, and 2E+Au (i.e., Pt+Pd+Au), in the context of Platreef ore flotation. Experimental tests were conducted on a Platreef ore feed using various dosages of depressants, frothers, and collectors under controlled agitation and pH conditions. The recoveries of the individual PGEs were analysed using six kinetic models, with the modified Kelsall model identified as the most suitable for accurately describing the flotation kinetics and predicting elemental recovery. Notably, the model incorporates two rate constants (k_{fast} and k_{slow}) to account for the distinct flotation behaviours of the PGEs. The results indicate that Pt has the fastest floatability, followed by Pd and 2E+Au. The modified Kelsall model demonstrates high effectiveness in predicting the recovery of these PGEs. Three empirical correlations for Pt, Pd, and 2E+Au recoveries based on the modified Kelsall model are proposed, enhancing the understanding and optimisation of PGE recovery in Platreef ore flotation.

Keywords: PGM species; PGE floatability; kinetic model; Platreef; recovery



Citation: Doubra, P.; Carelse, C.; Chetty, D.; Manuel, M. Experimental and Modelling Study of Pt, Pd, and 2E+Au Flotation Kinetics for Platreef Ore by Exploring the Influence of Reagent Dosage Variations. *Minerals* **2023**, *13*, 1350. <https://doi.org/10.3390/min13101350>

Academic Editors: Fardis Nakhaei, Ahmad Hassanzadeh, Luis A. Cisternas and Hyunjung Kim

Received: 13 September 2023

Revised: 9 October 2023

Accepted: 18 October 2023

Published: 23 October 2023



Copyright: © 2023 by the authors. Licensee MDPI, Basel, Switzerland. This article is an open access article distributed under the terms and conditions of the Creative Commons Attribution (CC BY) license (<https://creativecommons.org/licenses/by/4.0/>).

1. Introduction

Platinum group elements (PGEs) comprise a group of six metallic elements, namely, platinum, palladium, rhodium, ruthenium, iridium, and osmium [1,2]. These elements display common physical and chemical properties, including high melting points, resistance to wear and tear, and exceptional catalytic activity [3]. Due to their unique properties, PGEs are considered rare and valuable and find numerous applications in various industries such as automotive [4], aerospace [5], electronics [6,7], production of fertilisers [8], plastics [9], and pharmaceuticals [10].

PGEs make up platinum-group minerals (PGMs), and the latter are mainly found in deposits that are rich in nickel, copper, and other metals. The primary sources of PGMs are deposits in South Africa, Russia, and Canada, with smaller deposits being found in Zimbabwe, Australia, and the United States [11]. The Bushveld Complex in South Africa holds approximately 75% of the world's Pt resources and 50% of its Pd resources, with these precious metals being predominantly found in the Merensky, UG2, and Platreef layers [12,13]. The Platreef is a layered mafic-ultramafic intrusion located in the northern limb of the Bushveld Complex. This is a complex assemblage of different rock types, including serpentinites, pyroxenites, and calc-silicates, hosting predominantly PGE tellurides, alloys, arsenides, and sulphides. While Pt and Pd tellurides are the major contributors to the PGM assemblage, the Platreef is characterised by a scarcity of Pt-Pd sulphides compared with other reefs in the Bushveld Complex. The high concentration of telluride minerals in the Platreef is primarily represented by merenskyite and moncheite, whereas the arsenides are mainly composed of sperrylite and palladoarsenide [14–16].

The recovery of PGEs from the Platreef is achieved through flotation, a selective separation process based on differences in hydrophobicity of minerals [17]. Platreef ore

poses a challenge in flotation as the ore contains a larger proportion of fine-grained PGMs in association with gangue minerals compared with other reefs in the Bushveld Complex [18]. This disturbs the froth stability owing to the low mass and high surface area of fine particles [19], unlike Merensky ore, with a straightforward flotation process [18]. Froth stability in flotation is essential for effectively recovering valuable minerals and preventing the entrainment of gangue minerals during water recovery [20]. Consequently, the frother dosage is slightly higher (30–50 g/t) for Platreef ore due to froth instability and bubble challenges compared with other reefs. The overall floatability of valuable minerals in the ore results in varying collector requirements, where each collector performs a different action and therefore may target different sized particles [21].

The development of a kinetic model exclusively tailored through data-fit constants for Platreef ore flotation considering the reagents and test conditions stands as a significant advancement, distinct from UG2 and Merensky ores within the Bushveld Complex. This study aims at quantifying Pt, Pd, and 2E+Au (i.e., Pt+Pd+Au) behaviour through modelling the unique flotation response to variable reagent dosages for Platreef ore. By focusing solely on Platreef ore flotation, the model captures the intricacies and complexities inherent to this particular reef, allowing for the prediction of flotation behaviour.

The flotation behaviour of PGMs can be influenced by several factors, including the mineralogy (such as mineral association), particle size, reagent regime, and flotation conditions. The choice of flotation reagents and their concentrations can significantly affect the recovery of PGMs, and the effectiveness of these reagents may depend on the mineralogical attributes of the PGM species [22]. Flotation conditions, such as pH, temperature, and agitation rate, can also influence the recovery of PGMs [23–25].

In the early days of flotation, the initial flotation model developed by Gaudin [26] in the 1930s expressed flotation recovery as an exponential function of time. Since then, a range of flotation models has been proposed, published, and refined over time. These models often take into account various factors, including particle size, reagent chemistry, and process conditions, to predict flotation performance and optimise process efficiency [27]. They range from simple empirical equations to more complex and mechanistic formulations. The selection of an appropriate kinetic model for a given flotation experiment or plant depends on the specific conditions and objectives.

One key aspect of the flotation process is the rate at which the commodity of value is recovered. An example of a model to describe the rate is the first-order model, which assumes that the rate of mineral recovery decreases exponentially over time. Nonetheless, other models have also been developed based on the probability of particle–bubble collision, attachment, detachment, particle size distribution, and distribution of floatability [28–30]. In recent years, the growing knowledge of the sub-processes that occur in the flotation cell has led to the development of more efficient flotation models that are used for process analysis, simulation, and optimisation. These models can be used to predict the flotation performance of different materials and machine types, as well as to optimise the operating conditions for maximum recovery and grade. However, the application of these models in the plant is challenged by the uncertainties and complexities of industrial operations. Therefore, the development of accurate and reliable kinetic models is crucial for the optimisation of froth flotation in the mineral processing industry. Readers are referred to the review papers and theses cited here [27,31,32].

The prevailing scientific consensus holds that the flotation process is governed by a first-order kinetic model that is characterised by a dependence on particle concentration and a rate constant. This view has primarily been advanced in [33–35], among others [27]. To monitor and quantify the efficacy of this process, it is customary to evaluate the recovery of a specific component over time, known as R [12,36].

In practice, the most common approach for characterising each fraction involves using deterministic k - R_{max} pairs. This approach assumes that the flotation rate constants are deterministic and time-invariant for narrower fractions with respect to particle properties. However, such an approach may not be flexible enough to represent slow and sustained

increasing recovery trends that are often observed in flotation responses with slow-floating components. In addition, over-fitting can occur when using a large number of discrete rate constants to represent a category, especially when the number of model parameters is comparable to the number of experimental data points. The use of more flexible models to represent such responses [37–39] has thus been suggested.

The attachment of mineral particles to bubbles is a complex process that involves several physical and chemical mechanisms, including adsorption, desorption, and chemical reactions. These mechanisms can be described mathematically using various models, which typically involve a set of differential equations that describe the concentration of particles and reagents in the flotation cell as a function of time [40,41]. The efficiency and selectivity of the flotation process are usually evaluated by measuring mineral recoveries and enrichment ratios at specific flotation or residence times. However, in many cases, it is necessary to investigate the performance of the process over time [42]. This is achieved by analysing the kinetic response of the process, which is essentially the change in mineral concentrations or cumulative recovery over time. The kinetic response has several important applications in mineral processing, including determining the maximum achievable recoveries, comparing different flotation types, investigating the effects of various operating conditions, scaling up metallurgical results, designing flotation circuits, and simulating flotation processes [32,43–45]. This study presents a novel and comprehensive investigation into the flotation kinetics of Pt, Pd, and 2E+Au based on experimental studies [46] using Platreef ore samples. The optimised parameters for the dosage of depressant, frother, and collector, as well as the monitoring of agitation rate and pH under different reagent conditions, allowed for a thorough and detailed assessment of the flotation performance. This paper is the first ever study to predict individual PGE flotation kinetics for the Platreef ore, achieving strong predictability despite the complex nature of the ore body as well as the reagent dosages. Notably, the most successful model demonstrated excellent capability for extrapolation.

2. Materials and Methods

2.1. Materials

A detailed description of the materials, methods, and experimental procedure is outlined in [46]. The chemicals employed in this investigation consisted of a frother (Senfroth522), depressant (Sendep30E), and collector (sodium isobutyl xanthate (SIBX) obtained from SENMIN. The Platreef ore feedstock was derived from a 100 kg bulk sample originating from the southern Platreef deposit.

2.2. Experimental Equipment and Procedure

The schematic of the experimental set-up is displayed in Figure 1. The experimental apparatus used in this study comprised a D12 Denver flotation machine with a cell capacity of 2.5 L. The cell was equipped with mechanical agitators to ensure uniform pulp mixing and an aeration system for controlled air bubble introduction with airflow measurements using a rotameter. This employs a linear scale, wherein 100% corresponds to an airflow rate of 21 NL/min at an absolute line pressure of 4.85 bar. This system is equipped with a pressure regulator to facilitate control. The incoming air is subjected to filtration through an in-line air cleaner, serving to inhibit the ingress of particulate matter and oil contaminants originating from the air compressor, thus safeguarding the integrity of the flotation cell [47]. Furthermore, a reagent addition system allowed precise dosing of chemicals. Within this configuration, the overflow from each test was designated as the rougher concentrate (RC), representing the fraction enriched with the desired minerals. Conversely, the collective effluent from the final experiment constituted the rougher tailing (RT), encompassing the particles that did not respond favourably to the flotation process. All products (concentrates and tails) were dried, and a sub-sample was split out for subsequent chemical analysis and mineralogical analysis. The samples were analysed using inductively coupled plasma

atomic emission spectroscopy (ICP-OES), and the mineral liberation of PGMs was obtained using a mineral liberation analyser (MLA).

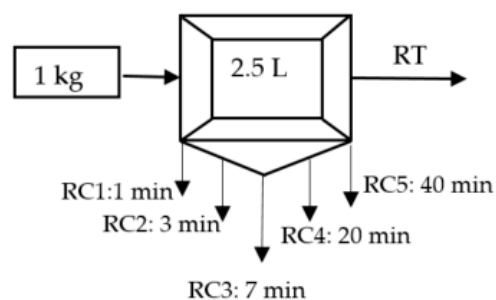


Figure 1. Schematic of the flotation set-up used in this work.

The behaviour of individual PGM species was investigated by liberating PGM grains from Platreef ore through fine grinding of the feed sample to 90% passing 75 μm . This fine grind was selected as the flotation response of liberated PGE species and was the focal point of our study. The Platreef feed sample contained PGE with a grade of approximately 2.8 g/t 2E (Au = 0.12 g/t, Pd = 1.61 g/t, and Pt = 1.17 g/t). The ore was subsequently crushed to 100% passing 1.7 mm using a jaw crusher and cone crusher, and 1 kg sub-samples were obtained using a rotary splitter for flotation test work.

Flotation test work was performed at a solids concentration of 35% and an impeller speed of 1200 rpm with a constant airflow. Tap water from the South African Rand Water supplier was used as the flotation medium. Table 1 presents the levels of cations, anions, conductivity, total dissolved solids (TDS), and pH identified in the tap water used for this study.

Table 1. Concentrations of selected ions in the sampled water [46].

Ions	Concentrations/ppm	Ions	Concentrations/Unit
Ag	<1	Si	<0.05 (ppm)
Al	<1	Li	<0.05 (ppm)
Ca	26.6	K	1.91 (ppm)
Cr	0.05	NO ₃ ⁻	5.14 (ppm)
Fe	0.51	Sulphide S	<0.05 (mg/L)
Mg	7.55	Conductivity	227 (uS/cm)
Pb	0.061	TDS	113.8 (mg/L)
V	0.06	pH	8.02

To investigate the response of individual liberated PGM species, reduced collector, depressant, and frother, dosages were tested. Figure 2 shows backscattered electron images of liberated PGM in the feed and concentrate.

The impact of the collector dosage on the recovery and flotation kinetics of PGEs was studied, while the frother's indirect effect was examined through froth phase effects. The reagents used and conditioning times are presented in Table 2. SIBX was introduced, and the slurry underwent a 2-min conditioning period. Sendep30E was added, and conditioning continued for an additional 3 min. Lastly, Senfroth522 was introduced, and the slurry underwent a final 1-min conditioning stage. The concentrate was manually collected by scraping once every 15 s using paddles.

Five timed RCs and an RT were produced from each test to ensure the reproducibility and statistical significance of the result. After each stage, an RC was collected, resulting in five rougher concentrates obtained at different cumulative flotation times of 1, 3, 7, 20, and 40 min, respectively (Table 2). Flotation progressed, resulting in the recovery of RC1 at 1 min, RC2 at 3 min after RC1 was taken, RC3 at 7 min after RC2, RC4 at 20 min after RC3, and RC5 at 40 min.

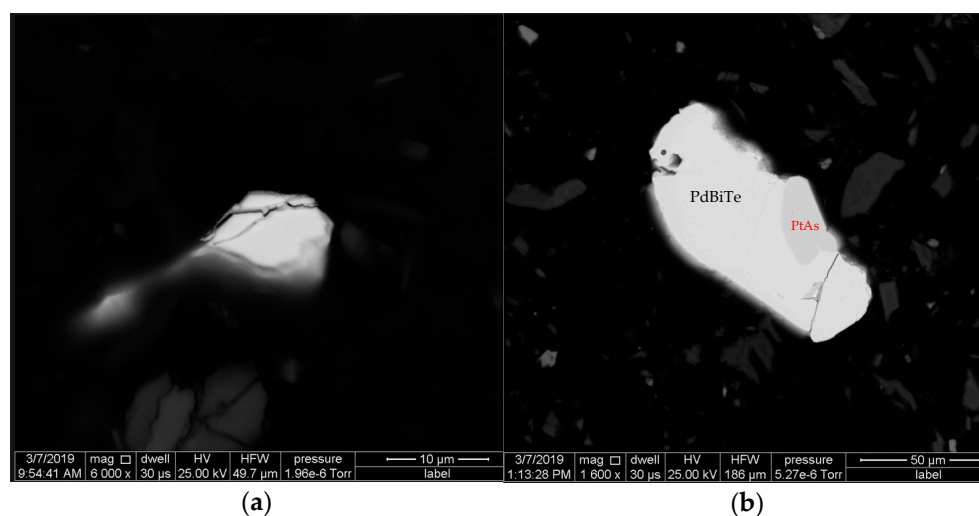


Figure 2. Backscattered electron image of (a) PtAs in the feed and (b) PdBiTe associated with PtAs in RC1.

Table 2. Platreef sample flotation test conditions.

Reagents & Dosages	Conditioning Time/min	Float Time/min
SIBX: 30 and 120 g/t	2	-
Sendep30E: 300 and 500 g/t	3	-
Senfroth522: 30 and 50 g/t	1	-
Rougher concentrate 1 (RC1)	-	1
Rougher concentrate 2 (RC2)	-	3
Rougher concentrate 3 (RC3)	-	7
Rougher concentrate 4 (RC4)	-	20
Rougher concentrate 5 (RC5)	-	40

The rougher flotation circuit is a vital component of the mineral processing circuit since it aims to achieve maximum recovery of valuable minerals from the feed material. Consequently, understanding the behaviour of PGM minerals during rougher flotation was crucial for optimising the overall recovery and efficiency of the mineral processing circuit.

2.3. Modelling

Various kinetic models have been studied to produce a comparative overview of their performance and to develop an accurate predictive tool. Flotation modelling has become increasingly sophisticated, with more advanced models being developed to incorporate additional complexities, such as the effect of particle size, the impact of froth zone turbulence, and the influence of inter-particle forces. However, the batch flotation models presented in this table remain highly relevant, especially in the context of the rougher stage of flotation processes.

Table 3 lists the flotation kinetic models parameterised in this study, including details on their equations, parameters, and associated references. The Classic, Klimpel, and second-order Klimpel models describe the mineral recovery over time in batch flotation processes, where R represents the recovery, k represents the flotation rate constant at which the minerals are recovered during the flotation process, t represents time, and R_{max} represents the species maximum recovery.

Table 3. Kinetic models for flotation separation.

Model Name	Equation	Kinetic Parameters	Ref.
Classical first-order model	$R = R_{max}(1 - e^{-Kt})$	R_{max} and k	[28]
Klimpel model	$R = R_{max} \left[1 - \frac{1}{k_{max}t} (1 - e^{-k_{max}t}) \right]$	R_{max} and k_{max}	[29]
Second-order	$R = \frac{R_{max}^2 k_{max}t}{1 + R_{max} k_{max}t}$	R_{max} and k_{max}	[28]
Second-order Klimpel	$R = R_{max} \left[1 - \frac{1}{k_{max}t} \ln(1 + k_{max}t) \right]$	R_{max} and k_{max}	[30]
Kelsall	$R = R_{fast} (1 - e^{-k_{fast}t}) + R_{slow} (1 - e^{-k_{slow}t})$	$100\% = R_{fast} + R_{slow}$ k_{slow} and k_{fast}	[47]
Modified Kelsall	$R = R_{fast} (1 - e^{-k_{fast}t}) + R_{slow} (1 - e^{-k_{slow}t})$	$R_{max} = R_{fast} + R_{slow}$ k_{slow} and k_{fast}	[33,34]

In the Kelsall and modified Kelsall models, R_{fast} and R_{slow} represent the fractions of species undergoing fast and slow flotation, respectively, while k_{fast} and k_{slow} denote the corresponding fast and slow flotation rate constants. In the Kelsall model, species are categorised as either fast or slow floaters, ensuring that the combined fractions of these species always amount to 100%, as demonstrated in Equation (1). However, in the modified Kelsall model, the sum of these fractions corresponds to R_{max} , signifying the maximum recoverable fraction of species, as depicted in Equation (2):

$$R_{fast} + R_{slow} = 100\%, \tag{1}$$

$$R_{fast} + R_{slow} = R_{max}. \tag{2}$$

The provided flotation models were assessed to gauge their accuracy in predicting the behaviour of PGEs, including Pt, Pd, and 2E+Au. To evaluate their performance, each model was fitted to experimental data to obtain the most appropriate kinetic parameters. The effectiveness of each model was subsequently determined by comparing its projected flotation kinetics with the actual kinetics observed during laboratory testing.

2.4. Statistical Analysis

In statistical evaluation, R-squared (R^2) and root mean squared error (RMSE) were used to assess the effectiveness of regression models. The formula used to calculate R^2 is given in Equation (3):

$$R^2 = 1 - \frac{RSS}{TSS}, \tag{3}$$

where RSS is the sum of the squared residuals (the difference between actual and predicted values), and TSS is the total sum of squares (the difference between actual values and the mean value). The formula used to calculate $RMSE$ is shown in Equation (4):

$$RMSE = \sqrt{\sum_{i=1}^N (z_{fi} - z_{oi})^2 / N}. \tag{4}$$

Here, z_{fi} is the predicted value, z_{oi} is the actual value, N is the number of observations in the dataset, and the sum is taken over all observations.

3. Results and Discussion

Regression analysis was used to determine the best data fit model among the models listed above that could provide a quantitative understanding of the underlying mechanisms that influence the flotation process. The residual study, a statistical method used to assess the accuracy of the models, was used to evaluate the goodness of fit of the models.

3.1. Experimental Results

Table 4 provides the recovery percentages of the three elements—Pt, Pd, and Au—at different stages of flotation using different combinations of collector, frother, and depressant. Table 4 focuses on the cumulative recovery percentage. For example, at 4 min (1+3 min), the recovery data are collected from both rougher concentrate 1 (collected after 1 min) and rougher concentrate 2 (collected after 3 min). Recovery is defined as the percentage of the valuable elements present in the ore that is recovered to the concentrate product. The outcomes indicate that the overall Pt recovery remains stable under diverse test conditions, whereas the recovery percentages for Pd are impacted by variations in reagent dosages. The optimal Pd recovery of 86.27% is achieved under the experimental parameters of 30 g/t collector, 30 g/t frother, and 300 g/t depressant.

Table 4. Impact of collector, frother, and depressant concentrations on the flotation performance of Platreef ore with cumulative times of 1, 4, 11, 31, and total of 40 min for the tests from RC1 to RC1+2+3+4+5, respectively.

Cumulative	Platinum %	Palladium %	2E + Au %
Collector 120 g/t, frother 50 g/t, and depressant 300 g/t			
RC1	55.44	52.28	52.13
RC1+RC2	72.63	68.64	68.37
RC1+RC2+RC3	78.45	75.48	74.56
RC1+RC2+RC3+RC4	83.57	80.99	79.74
RC1+RC2+RC3+RC4+RC5	86.96	84.64	83.16
Collector 30g/t, frother 50 g/t, and depressant 300 g/t			
RC1	56.69	53.57	56.01
RC1+RC2	72.76	69.70	71.39
RC1+RC2+RC3	78.96	76.54	77.68
RC1+RC2+RC3+RC4	84.59	82.05	83.06
RC1+RC2+RC3+RC4+RC5	86.84	84.62	85.45
Collector 120 g/t, frother 30 g/t, and depressant 300 g/t			
RC1	67.65	56.50	62.16
RC1+RC2	77.40	69.43	73.21
RC1+RC2+RC3	80.89	75.06	77.71
RC1+RC2+RC3+RC4	84.38	79.39	81.57
RC1+RC2+RC3+RC4+RC5	86.81	82.43	84.29
Collector 120 g/t, frother 50 g/t, and depressant 500 g/t			
RC1	60.87	46.23	53.21
RC1+RC2	74.45	63.27	68.35
RC1+RC2+RC3	79.55	70.57	74.48
RC1+RC2+RC3+RC4	83.88	77.53	80.10
RC1+RC2+RC3+RC4+RC5	86.72	81.92	83.71
Collector 30 g/t, frother 30 g/t, and depressant 300 g/t			
RC1	64.32	57.03	60.32
RC1+RC2	73.98	70.40	72.01
RC1+RC2+RC3	79.51	76.99	78.12
RC1+RC2+RC3+RC4	83.71	82.47	83.03
RC1+RC2+RC3+RC4+RC5	86.63	86.27	86.43

As expected, the results reveal that the selection of collector, frother, and depressant can significantly impact the recovery of the valuable elements. This is likely due to better selectivity achieved at the lower collector concentration. The higher dosage of SIBX is more applicable to UG2; compared with Platreef, UG2 ore may require a slightly higher dosage due to the limited floatability of valuable mineral species in combination with a co-collector such as dithiophosphate [19]. In contrast, the Platreef ore's complex composition may

contain Pd minerals with a high affinity for collectors, allowing for effective flotation at lower dosages. To address the issue of higher gangue recovery, many operations have opted to utilise higher concentrations of depressants [48]. However, increasing the depressant concentration from 300 g/t to 500 g/t with the same collector and frother dosage resulted in a decrease in recovery for Pd, likely due to the excessive use of depressant, leading to hindered collector attachment and froth destabilisation. In this context, the disparities in Pt concentrations are insignificant.

3.2. Kinetic Model

Figure 3 presents recovery percentages of Pt and Pd at various flotation stages, using different combinations of collector, frother, and depressant. Appendix A contains extra model results for 2E+Au. The results reveal distinct variations in the floatability of these PGEs. Among the models employed, the modified Kelsall model exhibited remarkable performance, demonstrating high R_{max} values and yielding excellent R^2 and low RMSE values (Table 5). The recovery percentages on the graphs have been adjusted to enhance visibility within the range of 45–85%, and the graphs commence from an initial recovery of zero at time zero. This suggests that the modified Kelsall model accurately captured the flotation kinetics and proved effective in predicting the floatability of Pt and Pd. Notably, Pt demonstrated favourable floatability, as indicated by its high R_{max} value and the model's robust fit. Pd exhibited slightly lower R_{max} values but still demonstrated good flotation response according to the model.

Table 5. Modified Kelsall model for PGE recovery.

Modified Kelsall	R_{max}	R_{fast}	$k_{fast} \text{ min}^{-1}$	$k_{slow} \text{ min}^{-1}$	R^2	RMSE
Collector 120 g/t, frother 50 g/, and depressant 300 g/t						
Pt	0.888	0.700	1.52	0.050	0.99822	0.006
Pd	0.856	0.646	1.561	0.060	0.99758	0.005
2E+Au	0.844	0.649	1.543	0.056	0.99787,	0.005
Collector 30 g/t, frother 50 g/t, and depressant 300 g/t						
Pt	0.874	0.683	1.668	0.071	0.99935	0.002
Pd	0.849	0.646	1.6411	0.077	0.99886	0.002
2E+Au	0.859	0.668	1.706	0.073	0.99910	0.001
Collector 120 g/t, frother 30 g/t, and depressant 300 g/t						
Pt	0.895	0.758	2.170	0.037	0.99900	0.001
Pd	0.829	0.659	1.841	0.063	0.99785	0.002
2E+Au	0.855	0.708	2.025	0.051	0.99842	0.001
Collector 120 g/t, frother 50 g/t, and depressant 500 g/t						
Pt	0.877	0.715	1.827	0.056	0.99846	0.002
Pd	0.859	0.651	1.618	0.049	0.99741	0.011
2E+Au	0.859	0.651	1.618	0.049	0.99790	0.005
Collector 30 g/t, frother 30 g/t, and depressant 300 g/t						
Pt	0.870	0.704	2.293	0.066	0.99796	0.000
Pd	0.876	0.666	1.826	0.056	0.99730	0.002
2E+Au	0.873	0.683	2.018	0.060	0.99758	0.001

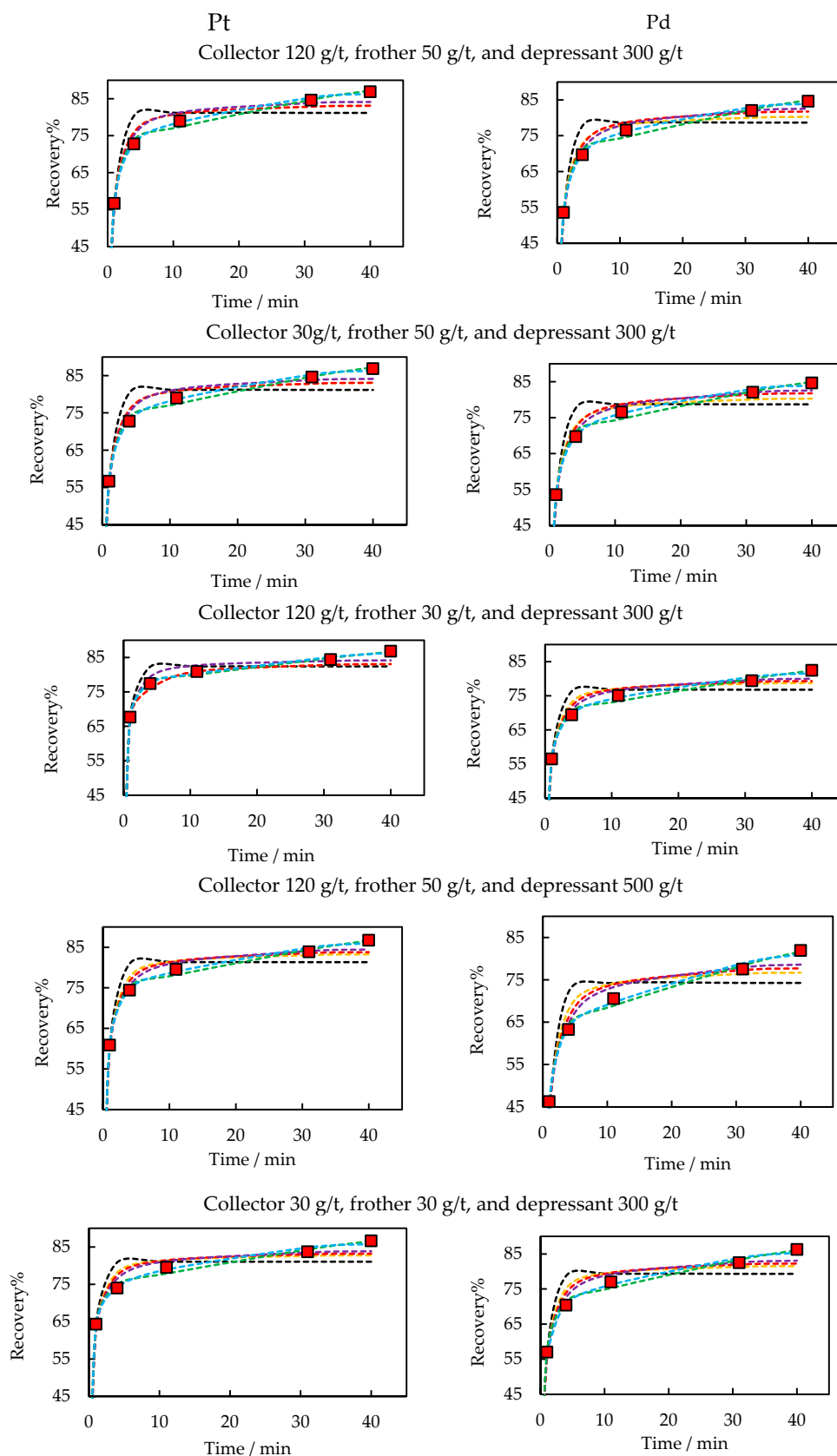


Figure 3. PGEs recovery data fit results for Pt and Pd, using different combinations of collector, frother, and depressant. ■ Experimental data; --- classic model; Klimpel model; -.- second order, --- second-order Klimpel; -.- Kelsall; and -.- modified Kelsall.

3.3. Model Extrapolation Performance

Table 5 presents parameters and statistics for the modified Kelsall model under different reagent conditions. Additional model results are provided in Appendix A. The modified Kelsall model's high R_{max} values for Pt, Pd, and 2E+Au suggest efficient recovery due to favourable floatability. It effectively captures flotation kinetics, offering insights into particle attachment and detachment. The modified Kelsall model demonstrates accuracy in predicting Pt, Pd, and 2E+Au flotation in Platreef ore with strong correlations (R^2) and low RMSE values. The R_{fast} for Pt exhibits the highest floatability, followed by 2E+Au and Pd. Pd-bearing minerals are found to be more oxidised than Pt-bearing minerals, which could be a contributing factor since they offer fewer active sites for collector adsorption [49].

Based on Ramlall, the flotation for 2E+Au in the UG2 deposit involved the use of SIBX as collector at 150 g/t, KU5 as frother at 30 g/t, and dowfroth 200 as depressant at 20 g/t [31,47]. The high value of R_{max} (88.26%) suggests efficient flotation recovery, indicating the successful separation of the valuable 2E+Au. In the flotation tests for Platreef ore, different reagents were utilised compared to UG2, including different combinations of collector, frother, and depressant. The highest achieved recovery (R_{max}) of 87.60% in Platreef ore was observed for 2E+Au under the optimal variable conditions, including collector at 30 g/t, frother at 30 g/t, and depressant at 300 g/t. The flotation testing results for 2E+Au in UG2 and Platreef indicate successful separation of the valuable minerals using various reagent combinations.

Irrespective of different reagents and dosages in the tests, for Platreef ore, R_{max} was determined as 0.873, comprising 0.68 R_{fast} and 0.19 R_{slow} . In contrast, UG2 ore demonstrated a higher R_{max} of 0.8826, divided into 0.62 R_{fast} and 0.26 R_{slow} [31,47]. UG2 ore demonstrated a slightly higher overall recovery compared with Platreef ore. Moreover, Platreef ore exhibited a higher proportion of fast-floating particles, while UG2 ore demonstrated a larger fraction of slow-floating species.

For the Platreef ore, the rate constant values for 2E+Au at the optimum condition of collector 30 g/t, frother 30 g/t and depressant 300 g/t are calculated as $k_{fast} = 2.02 \text{ min}^{-1}$ and $k_{slow} = 0.06 \text{ min}^{-1}$. In contrast, the UG2 ore demonstrates higher rate constant values, with $k_{fast} = 2.26 \text{ min}^{-1}$ and $k_{slow} = 0.13 \text{ min}^{-1}$. Platreef ore exhibits a comparatively lower k_{fast} , indicating a slower initial attachment of particles to bubbles. Conversely, UG2's higher k_{fast} points to a swifter initial particle–bubble interaction. The variance in k_{slow} values mirrors a similar trend: Platreef ore presents a relatively lower rate of slow flotation compared to UG2, which is affected by the differences in the mineralogy of the two ores as mentioned in the introduction.

The study on recovering Pt, Pd, and 2E+Au from Platreef ore has identified the modified Kelsall model as the most fitting model for the system, among others tested. The modified Kelsall model's superior performance is attributed to its ability to capture the nuances of the flotation process through its incorporation of two rate constants, k_{fast} and k_{slow} , which describe the flotation behaviour of two distinct fast and slow floating populations. The model's success is also due to its balance between accuracy and complexity. Despite its increased complexity compared to alternative models, the modified Kelsall model remains interpretable and practical, making it an ideal tool for both understanding the flotation of Platreef ore and optimising process conditions. Moreover, the model's capacity to handle changes in reagent conditions tested for Platreef ore more effectively than other models likely contributes to its enhanced accuracy in representing the flotation process. Generally, higher k values suggest faster flotation kinetics. In this case, the k values for the three elements are relatively consistent across the different tests, indicating that the flotation kinetics are not significantly affected by the changes in reagent dosages.

Table 6 lists three empirical correlations based on the modified Kelsall model to predict the flotation of individual PGEs/PGE groupings from Platreef ore for the frother, collector and depressant dosages in the ranges of 30–50, 30–120, and 300–500 g/t, respectively. Figure 4 depicts the recovery data fit results of modified Kelsall for Pt under all the conditions tested. In the case of the Platreef ore, a depressant dosage of 300 g/t of

Sendep suppresses gangue minerals with stronger flotation tendencies. An elevated dosage improves inhibition, thereby enhancing selectivity for valuable minerals.

Table 6. Empirical correlation based on modified Kelsall model to predict the flotation of individual PGEs/PGE groups from Platreef ore for the collector, frother, and depressant dosage ranges of 30–120, 30–50, and 300–500 g/t.

PGEs	Model
Pt	$R = 0.71(1 - e^{-1.86t}) + 0.17(1 - e^{-0.06t})$
Pd	$R = 0.64(1 - e^{-1.65t}) + 0.21(1 - e^{-0.06t})$
2E+Au	$R = 0.67(1 - e^{-1.77t}) + 0.18(1 - e^{-0.06t})$

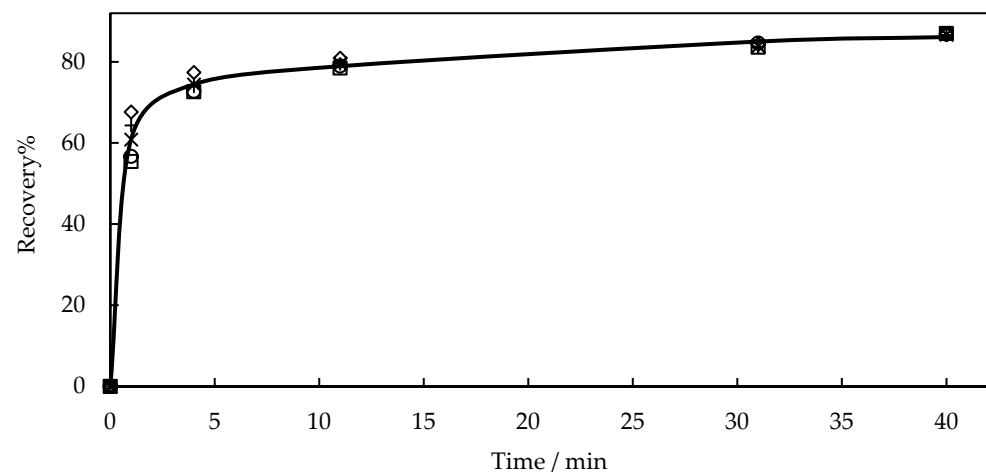


Figure 4. Recovery data fit results of Pt for all the conditions tested. — modified Kelsall; depressant, collector, and frother concentrations of □ 300, 120, and 50; ○ 300, 30, and 50; ◆ 300, 50, and 30; × 500, 120, and 50; and + 300, 120, and 50.

The ability of the modified Kelsall model to accurately describe the data as per findings here suggests that it is an appropriate model for predicting metal recovery from Platreef ore under different reagent dosage conditions. Moreover, the residual analysis of the data demonstrated that the modified Kelsall model fitted in this study was able to extrapolate results beyond the range of the data used to fit the model, while the precision of predictions requires further consideration. While the model's predictions consistently approximate the true value, an asymmetrical distribution of error values and deviation from the mean indicates a lack of precision in predictions.

Figure 5 depicts the scatter of residuals as red rings, which provide a one-sided representation of the deviation from the precision of the data fit model in relation to experimental results. The relatively small error figures suggest that a single correlated modified Kelsall model is highly accurate overall. However, this finding implies that the model may not be able to make precise predictions for extended flotation tests, which can be a critical aspect of mineral processing optimisation.

Figures 6–9 showcase the recovery and residuals for Pd and 2E+Au species. Despite the observed deviations for Pt (see Figure 3), the modified Kelsall model has exhibited superior performance in these instances, with the residuals scattering randomly around both sides of the coordinates.

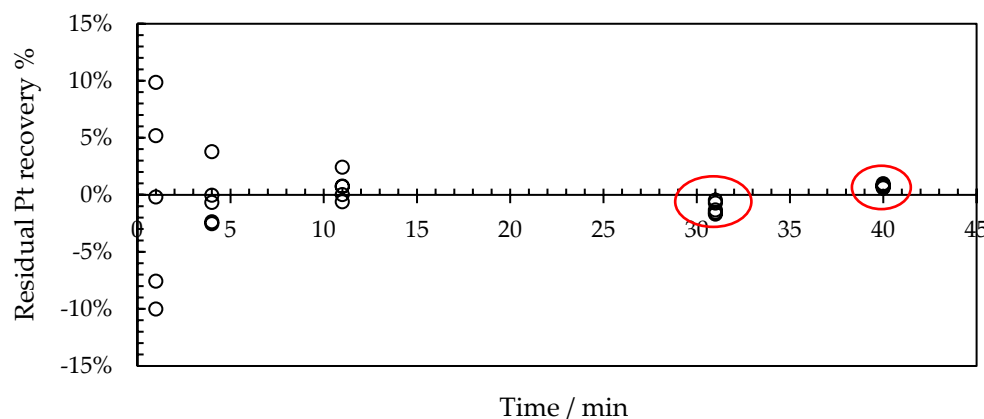


Figure 5. Residual study of modified Kelsall model for Pt recovery in five different tests. ○ Discrepancies associated with each data point when compared to experimental measurements.

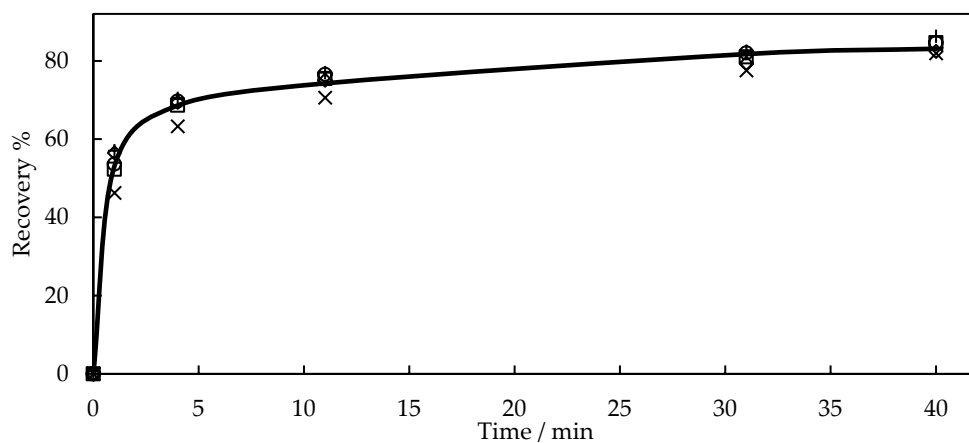


Figure 6. Recovery data fit results of Pd for all the tested conditions: — modified Kelsall; depressant, collector, and frother concentrations of □ 300, 120, and 50; ○ 300, 30, and 50; ◆ 300, 50, and 30; × 500, 120, and 50; and + 300, 120, and 50.

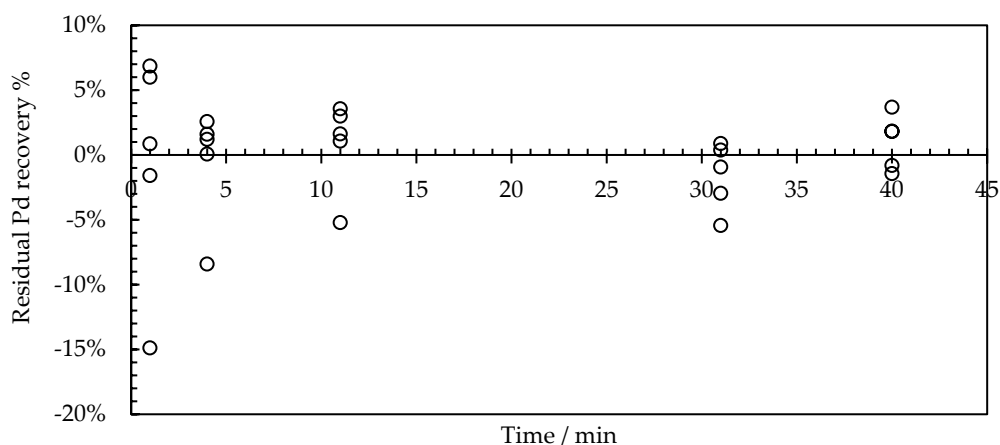


Figure 7. Residual study of modified Kelsall model Pd recovery in five different tests. ○ Discrepancies associated with each data point when compared to experimental measurements.

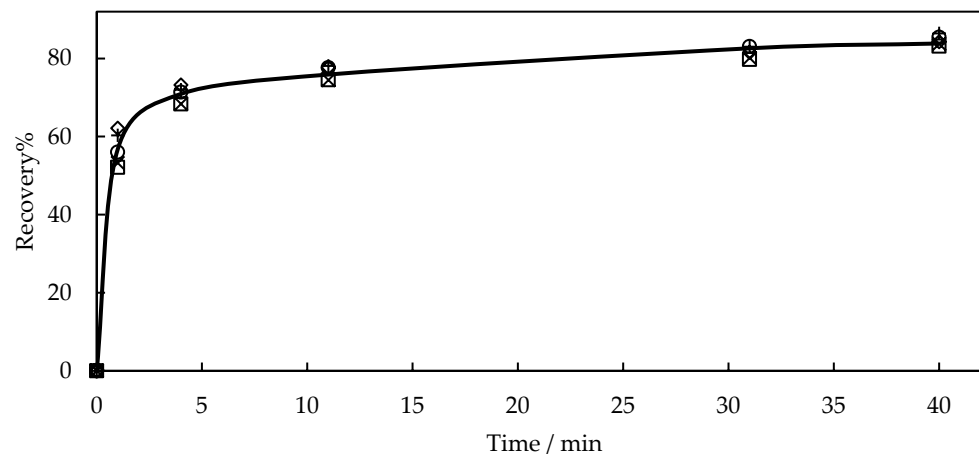


Figure 8. Recovery data fit results of 2E+Au for all the tested conditions: — modified Kelsall; depressant, collector, and frother concentrations of □ 300, 120, and 50; ○ 300, 30, and 50; ◆ 300, 50, and 30; × 500, 120, and 50; and + 300, 120, and 50.

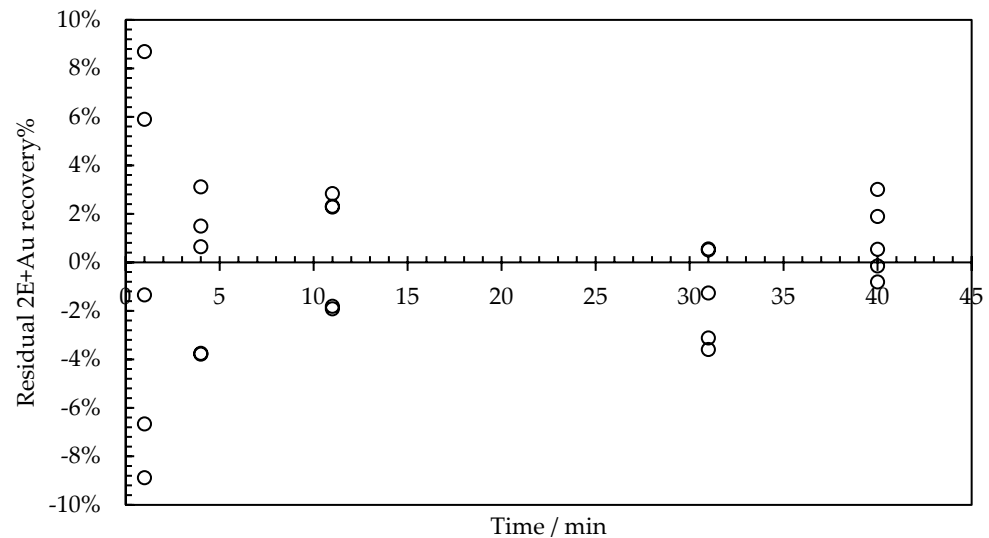


Figure 9. Residual study of modified Kelsall model 2E+Au recovery in five different tests. ○ Discrepancies associated with each data point when compared to experimental measurements.

4. Conclusions

Experimental data were generated for the flotation of Platreef ore using various depressant, frother, and collector dosages at a controlled agitation rate, and the recoveries of individual PGE (Pt, Pd, 2E+Au) have been analysed using six different kinetic models. The modified Kelsall model was found to be the most suitable model for accurately describing the kinetics of the flotation process and predicting metal recovery under different reagent dosage conditions. The model's ability to account for the distinct flotation behaviours of two distinct PGE, viz., Pt and Pd, as well as 2E+Au, through the incorporation of two rate constants, k_{fast} and k_{slow} , is a significant advantage in modelling the complex Platreef ore flotation system. The findings suggest that Pt has the fastest floatability, followed by Pd and 2E+Au. Pd minerals, with higher oxidation levels, may have fewer active adsorption sites, possibly accounting for the collector adsorption difference compared to Pt minerals.

The modified Kelsall model is a highly effective method among models studied for predicting the recovery of Pt, Pd, and 2E+Au from Platreef ore through flotation. The residual analysis approach enabled the refinement of the model and increased confidence in its ability to accurately predict data outside the range of the training data. Three empirical correla-

tions following the modified Kelsall model were proposed for Pt, Pd, and 2E+Au recoveries, making this a novel advancement for Platreef ore flotation performance prediction.

Author Contributions: Conceptualization, all authors.; methodology, all authors.; software, P.D.; validation, all authors.; formal analysis, P.D.; investigation, P.D. and C.C.; data curation, P.D. and C.C.; writing—original draft preparation, P.D.; writing—review and editing, all authors.; visualization, P.D.; supervision, D.C. and M.M.; project administration, C.C.; funding acquisition, C.C. All authors have read and agreed to the published version of the manuscript.

Funding: Funding for this work was provided via Mintek’s Science Vote Grant.

Data Availability Statement: All data have been provided in the manuscript and Appendix A.

Acknowledgments: The authors would like to thank Mintek for providing financial support to this project. Colleagues in the Minerals Processing Division are acknowledged for conducting the flotation tests.

Conflicts of Interest: The authors declare no conflict of interest.

Appendix A

The test conditions are summarised in Table A1 and represented in Figures A1–A5.

Table A1. Experimental flotation tests on the Platreef samples with different reagent dosing.

Test No.	Depressant ¹	Collector ¹	Frother ¹	Mixer Rate ²	pH	Representation
1	300	120	50			Figure A1
2	300	30	50			Figure A2
3	300	120	30	1200 (all tests)	9 (all tests)	Figure A3
4	500	30	50			Figure A4
5	500	30	30			Figure A5

¹ Reagent concentration in g/t. ² Mixer rate in rpm.

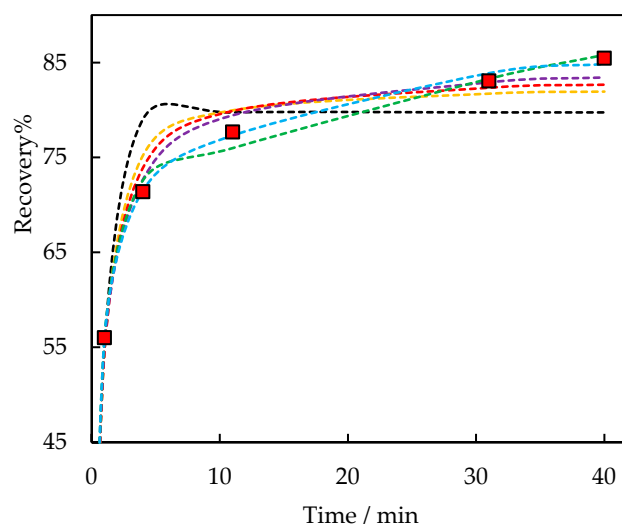


Figure A1. PGE recovery data fit results 2E+Au with depressant, collector, and frother concentrations of 300, 120, and 50 g/t, respectively. ■ Experimental data; --- classic model; --- Klimpel model; --- second order, --- second-order Klimpel; --- Kelsall; and --- modified Kelsall.

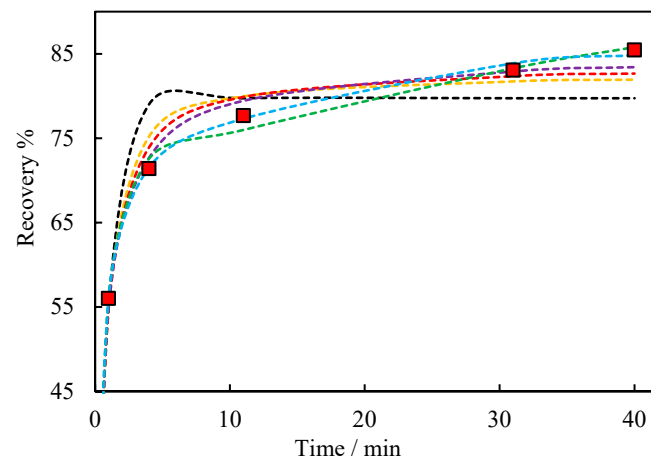


Figure A2. Recovery data fit results 2E+Au with depressant, collector, and frother concentrations of 300, 50, and 30 g/t, respectively. ■ Experimental data; --- classic model; --- Klimpel model; --- second order, --- second-order Klimpel; --- Kelsall; and --- modified Kelsall.

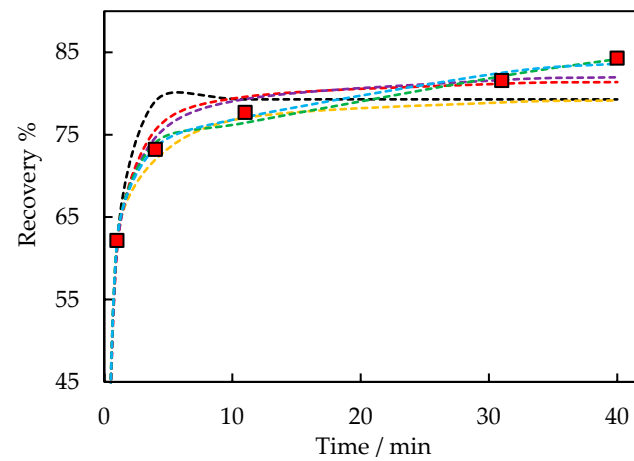


Figure A3. Recovery data fit results 2E+Au with depressant, collector, and frother concentrations of 300, 120, and 30 g/t, respectively. ■ Experimental data; --- classic model; --- Klimpel model; --- second order, --- second-order Klimpel; --- Kelsall; and --- modified Kelsall.

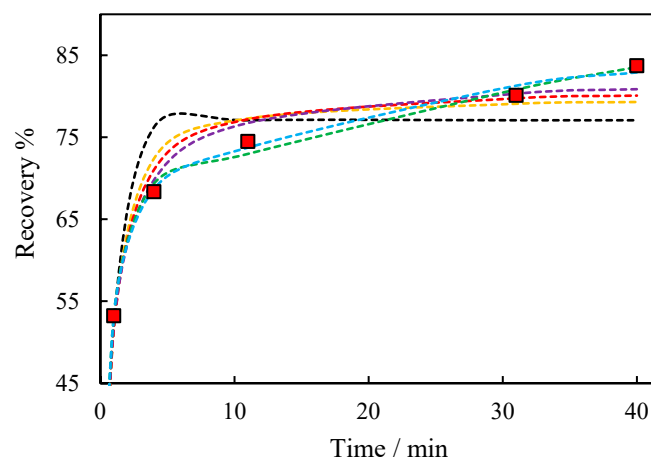


Figure A4. Recovery data fit results 2E+Au with depressant, collector, and frother concentrations of 500, 120, and 50 g/t, respectively. ■ Experimental data; --- classic model; --- Klimpel model; --- second order, --- second-order Klimpel; --- Kelsall; and --- modified Kelsall.

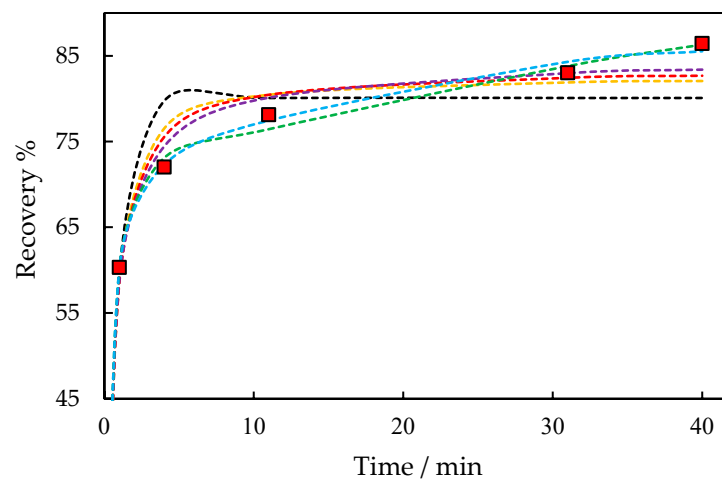


Figure A5. Recovery data fit results 2E+Au with depressant, collector, and frother concentrations of 300, 30, and 30 g/t, respectively. ■ Experimental data; --- classic model; --- Klimpel model; --- second order, --- second-order Klimpel; --- Kelsall; and --- modified Kelsall.

Table A2 presents PGE recovery data fit results of Pt, Pd, and 2E+Au with depressant, collector, and frother concentrations of 300, 120, and 50 g/t, respectively. The analysis of various flotation models for Pt, Pd, and 2E+Au in Platreef ore for this experimental condition reveals that the modified Kelsall model performs exceptionally well in predicting the flotation behaviour of these PGEs. The model exhibits high R_{max} values for Pt, Pd, and 2E+Au, indicating their favourable floatability and potential for efficient recovery. The model's ability to capture the kinetics of flotation, including fast and slow flotation rate constants, provides valuable insights into the attachment and detachment processes of PGM particles during flotation. With high correlation coefficients (R^2) and low root mean square error (RMSE) values, the modified Kelsall model (parameterised for this work) demonstrates its accuracy and reliability in predicting the flotation performance of Pt, Pd, and 2E+Au in Platreef ore. Overall, Pt demonstrates the highest floatability, followed by Pd and 2E+Au.

Table A3 presents recovery data fit results of Pt, Pd, and 2E+Au with depressant, collector, and frother concentrations of 30, 50, and 300 g/t, respectively. The results reveal distinct variations in the floatability of these PGEs. Among the models employed, the modified Kelsall model exhibited remarkable performance, demonstrating high R_{max} values and yielding excellent R^2 and low RMSE values. This suggests that the modified Kelsall model accurately captured the flotation kinetics and proved effective in predicting the floatability of Pt, Pd, and 2E+Au. Notably, Pt demonstrated favourable floatability, as indicated by its high R_{max} value and the model's robust fit. Pd exhibited slightly lower R_{max} values but still demonstrated good flotation response according to the model. On the other hand, 2E+Au displayed lower R_{max} values compared to Pt and Pd, indicating relatively lower floatability for this PGE group.

Table A4 presents PGE recovery data fit results of Pt, Pd, and 2E+Au with depressant, collector, and frother concentrations of 120, 30, and 300 g/t, respectively. Among the models employed, the modified Kelsall model exhibited excellent performance, with high R_{max} values, strong R^2 , and low RMSE values. This indicates the model's ability to accurately describe the flotation kinetics of Pt, Pd, and 2E+Au under condition 3. Notably, Pt displayed favourable floatability, as evidenced by its high R_{max} value and the robust fit obtained from the model. Pd exhibited slightly lower R_{max} values but still demonstrated good flotation response according to the model. In contrast, 2E+Au exhibited relatively lower R_{max} values compared to Pt and Pd, indicating reduced floatability for this PGE grouping under condition 3.

Table A2. PGE recovery data fit results (a) Pt, (b) Pd, and (c) 2E+Au with collector, frother, and depressant concentrations of 120, 50, and 300g/t, respectively.

Pt	
Classic	$R_{max} = 0.808, k = 1.119 \text{ min}^{-1}, R^2 = 0.92580, \text{RMSE} = 0.414$
Klimpel	$R_{max} = 0.839, k = 2.619 \text{ min}^{-1}, R^2 = 0.97588, \text{RMSE} = 0.509$
Second order	$R_{max} = 0.850, k = 2.077 \text{ min}^{-1}, R^2 = 0.98560, \text{RMSE} = 0.473$
Second-order Klimpel	$R_{max} = 0.870, k = 4.686 \text{ min}^{-1}, R^2 = 0.99281, \text{RMSE} = 0.275$
Kelsall	$R_{fast} = 0.717, k_{fast} = 1.448 \text{ min}^{-1}, k_{slow} = 0.019 \text{ min}^{-1}, R^2 = 0.99758, \text{RMSE} = 0.020$
Modified Kelsall	$R_{max} = 0.888, R_{fast} = 0.70, k_{fast} = 1.52 \text{ min}^{-1}, k_{slow} = 0.05 \text{ min}^{-1}, R^2 = 0.99822, \text{RMSE} = 0.006$
Pd	
Classic	$R_{max} = 0.780, k = 1.058 \text{ min}^{-1}, R^2 = 0.90703, \text{RMSE} = 0.560$
Klimpel	$R_{max} = 0.811, k = 2.427 \text{ min}^{-1}, R^2 = 0.96647, \text{RMSE} = 0.664$
Second order	$R_{max} = 0.824, k = 1.939 \text{ min}^{-1}, R^2 = 0.97979, \text{RMSE} = 0.650$
Second-order Klimpel	$R_{max} = 0.846, k = 4.153 \text{ min}^{-1}, R^2 = 0.98972, \text{RMSE} = 0.452$
Kelsall	$R_{fast} = 0.678, k_{fast} = 1.434 \text{ min}^{-1}, k_{slow} = 0.018 \text{ min}^{-1}, R^2 = 0.99614, \text{RMSE} = 0.027$
Modified Kelsall	$R_{max} = 0.856, R_{fast} = 0.646, k_{fast} = 1.561 \text{ min}^{-1}, k_{slow} = 0.060 \text{ min}^{-1}, R^2 = 0.99758, \text{RMSE} = 0.005$
2E+Au	
Classic	$R_{max} = 0.769, k = 1.086 \text{ min}^{-1}, R^2 = 0.91573, \text{RMSE} = 0.474$
Klimpel	$R_{max} = 0.799, k = 2.514 \text{ min}^{-1}, R^2 = 0.97094, \text{RMSE} = 0.574$
Second order	$R_{max} = 0.811, k = 2.063 \text{ min}^{-1}, R^2 = 0.98258, \text{RMSE} = 0.552$
Second-order Klimpel	$R_{max} = 0.832, k = 4.389 \text{ min}^{-1}, R^2 = 0.99127, \text{RMSE} = 0.360$
Kelsall	$R_{fast} = 0.677, k_{fast} = 1.434 \text{ min}^{-1}, k_{slow} = 0.016 \text{ min}^{-1}, R^2 = 0.99669, \text{RMSE} = 0.025$
Modified Kelsall	$R_{max} = 0.844, R_{fast} = 0.649, k_{fast} = 1.543 \text{ min}^{-1}, k_{slow} = 0.056 \text{ min}^{-1}, R^2 = 0.99787, \text{RMSE} = 0.005$

Table A3. PGE recovery data fit results (a) Pt, (b) Pd, and (c) 2E+Au with collector, frother, and depressant concentrations of 30, 50, and 300 g/t, respectively.

Pt	
Classic	$R_{max} = 0.812, k = 1.162 \text{ min}^{-1}, R^2 = 0.92237, \text{RMSE} = 0.382$
Klimpel	$R_{max} = 0.859, k = 2.757 \text{ min}^{-1}, R^2 = 0.97779, \text{RMSE} = 0.00$
Second order	$R_{max} = 0.853, k = 2.171 \text{ min}^{-1}, R^2 = 0.98509, \text{RMSE} = 0.543$
Second-order Klimpel	$R_{max} = 0.872, k = 4.945 \text{ min}^{-1}, R^2 = 0.99336, \text{RMSE} = 0.366$
Kelsall	$R_{fast} = 0.719, k_{fast} = 1.514 \text{ min}^{-1}, k_{slow} = 0.0197 \text{ min}^{-1}, R^2 = 0.99719, \text{RMSE} = 0.020$
Modified Kelsall	$R_{max} = 0.874, R_{fast} = 0.683, k_{fast} = 1.668 \text{ min}^{-1}, k_{slow} = 0.071 \text{ min}^{-1}, R^2 = 0.99935, \text{RMSE} = 0.002$
Pd	
Classic	$R_{max} = 0.787, k = 1.095 \text{ min}^{-1}, R^2 = 0.91489, \text{RMSE} = 0.4490$
Klimpel	$R_{max} = 0.819, k = 2.70 \text{ min}^{-1}, R^2 = 0.97530, \text{RMSE} = 0.00$
Second order	$R_{max} = 0.830, k = 2.033 \text{ min}^{-1}, R^2 = 0.98381, \text{RMSE} = 0.601$
Second-order Klimpel	$R_{max} = 0.851, k = 4.431 \text{ min}^{-1}, R^2 = 0.99285, \text{RMSE} = 0.408$
Kelsall	$R_{fast} = 0.691, k_{fast} = 1.453 \text{ min}^{-1}, k_{slow} = 0.018 \text{ min}^{-1}, R^2 = 0.99591, \text{RMSE} = 0.028$
Modified Kelsall	$R_{max} = 0.849, R_{fast} = 0.646, k_{fast} = 1.6411 \text{ min}^{-1}, k_{slow} = 0.077 \text{ min}^{-1}, R^2 = 0.99886, \text{RMSE} = 0.002$
2E+Au	
Classic	$R_{max} = 0.798, k = 1.174 \text{ min}^{-1}, R^2 = 0.91997, \text{RMSE} = 0.368$
Klimpel	$R_{max} = 0.827, k = 2.767 \text{ min}^{-1}, R^2 = 0.97316, \text{RMSE} = 0.552$
Second order	$R_{max} = 0.838, k = 2.238 \text{ min}^{-1}, R^2 = 0.98393, \text{RMSE} = 0.561$
Second-order Klimpel	$R_{max} = 0.857, k = 5.016 \text{ min}^{-1}, R^2 = 0.99264, \text{RMSE} = 0.394$
Kelsall	$R_{fast} = 0.707, k_{fast} = 1.532 \text{ min}^{-1}, k_{slow} = 0.018 \text{ min}^{-1}, R^2 = 0.99664, \text{RMSE} = 0.020$
Modified Kelsall	$R_{max} = 0.859, R_{fast} = 0.668, k_{fast} = 1.706 \text{ min}^{-1}, k_{slow} = 0.073 \text{ min}^{-1}, R^2 = 0.99910, \text{RMSE} = 0.001$

Table A4. PGE recovery data fit results (a) Pt, (b) Pd, and (c) 2E+Au with collector, frother, and depressant concentrations of 120, 30, and 300 g/t, respectively.

Model	Parameters
Pt	
Classic	$R_{max} = 0.824, k = 1.712 \text{ min}^{-1}, R^2 = 0.95475, \text{RMSE} = 0.047$
Klimpel	$R_{max} = 0.990, k = 3.00 \text{ min}^{-1}, R^2 = 0.98522, \text{RMSE} = 0.00$
Second order	$R_{max} = 0.847, k = 4.403 \text{ min}^{-1}, R^2 = 0.98621, \text{RMSE} = 0.342$
Second-order Klimpel	$R_{max} = 0.858, k = 4.686 \text{ min}^{-1}, R^2 = 0.99161, \text{RMSE} = 0.296$
Kelsall	$R_{fast} = 0.767, k_{fast} = 2.101 \text{ min}^{-1}, k_{slow} = 0.014 \text{ min}^{-1}, R^2 = 0.99879, \text{RMSE} = 0.002$
Modified Kelsall	$R_{max} = 0.895, R_{fast} = 0.758, k_{fast} = 2.170 \text{ min}^{-1}, k_{slow} = 0.037 \text{ min}^{-1}, R^2 = 0.99900, \text{RMSE} = 0.001$
Pd	
Classic	$R_{max} = 0.768, k = 1.304 \text{ min}^{-1}, R^2 = 0.92176, \text{RMSE} = 0.227$
Klimpel	$R_{max} = 0.794, k = 3.161 \text{ min}^{-1}, R^2 = 0.97113, \text{RMSE} = 0.485$
Second order	$R_{max} = 0.802, k = 2.752 \text{ min}^{-1}, R^2 = 0.98062, \text{RMSE} = 0.528$
Second-order Klimpel	$R_{max} = 0.819, k = 6.074 \text{ min}^{-1}, R^2 = 0.98958, \text{RMSE} = 0.413$
Kelsall	$R_{fast} = 0.689, k_{fast} = 1.677 \text{ min}^{-1}, k_{slow} = 0.014 \text{ min}^{-1}, R^2 = 0.99624, \text{RMSE} = 0.012$
Modified Kelsall	$R_{max} = 0.829, R_{fast} = 0.659, k_{fast} = 1.841 \text{ min}^{-1}, k_{slow} = 0.063 \text{ min}^{-1}, R^2 = 0.99785, \text{RMSE} = 0.002$
2E+Au	
Classic	$R_{max} = 0.793, k = 1.518 \text{ min}^{-1}, R^2 = 0.93867, \text{RMSE} = 0.101$
Klimpel	$R_{max} = 0.941, k = 2.759 \text{ min}^{-1}, R^2 = 0.97315, \text{RMSE} = 0.006$
Second order	$R_{max} = 0.821, k = 3.548 \text{ min}^{-1}, R^2 = 0.98561, \text{RMSE} = 0.431$
Second-order Klimpel	$R_{max} = 0.834, k = 8.474 \text{ min}^{-1}, R^2 = 0.99007, \text{RMSE} = 0.361$
Kelsall	$R_{fast} = 0.726, k_{fast} = 1.902 \text{ min}^{-1}, k_{slow} = 0.014 \text{ min}^{-1}, R^2 = 0.99768, \text{RMSE} = 0.005$
Modified Kelsall	$R_{max} = 0.855, R_{fast} = 0.708, k_{fast} = 2.025 \text{ min}^{-1}, k_{slow} = 0.051 \text{ min}^{-1}, R^2 = 0.99842, \text{RMSE} = 0.001$

Table A5 presents recovery data fit results of Pt, Pd, and 2E+Au with depressant, collector, and frother concentrations of 120, 50, and 500 g/t, respectively. Among the models applied, the modified Kelsall model demonstrated superior performance, exhibiting high R_{max} values, strong R^2 , and low RMSE values. This indicates the model's effectiveness in describing the flotation kinetics of Pt, Pd, and 2E+Au under this test condition. Notably, Pt displayed favourable floatability, as evidenced by its high R_{max} value and the excellent fit obtained from the model. Pd exhibited slightly lower R_{max} values but still exhibited satisfactory flotation response according to the model. In contrast, 2E+Au exhibited relatively lower R_{max} values compared to Pt and Pd, suggesting reduced floatability for this PGE grouping.

Table A6 presents recovery data fit results of Pt, Pd, and 2E+Au with depressant, collector, and frother concentrations of 120, 50, and 500 g/t, respectively. Among the models applied, the modified Kelsall model exhibited excellent performance, demonstrating high R_{max} values, strong R^2 , and low RMSE values. This indicates the effectiveness of the model in describing the flotation kinetics of Pt, Pd, and 2E+Au. Pt displayed favourable floatability, as evidenced by its high R_{max} value and the excellent fit obtained from the model. Pd exhibited slightly lower R_{max} values but still demonstrated satisfactory flotation response according to the model. 2E+Au exhibited relatively lower R_{max} values compared to Pt and Pd, indicating its reduced floatability.

Table A5. PGE recovery data fit results of (a) Pt, (b) Pd, and (c) 2E+Au with collector, frother, and depressant concentrations of 120, 50, and 500 g/t, respectively.

Pt	
Classic	$R_{max} = 0.813, k = 1.359 \text{ min}^{-1}, R^2 = 0.93434, \text{RMSE} = 0.181$
Klimpel	$R_{max} = 0.839, k = 3.369 \text{ min}^{-1}, R^2 = 0.97721, \text{RMSE} = 0.421$
Second order	$R_{max} = 0.847, k = 2.834 \text{ min}^{-1}, R^2 = 0.98469, \text{RMSE} = 0.450$
Second-order Klimpel	$R_{max} = 0.863, k = 6.731 \text{ min}^{-1}, R^2 = 0.99200, \text{RMSE} = 0.333$
Kelsall	$R_{fast} = 0.737, k_{fast} = 1.712 \text{ min}^{-1}, k_{slow} = 0.017 \text{ min}^{-1}, R^2 = 0.99756, \text{RMSE} = 0.009$
Modified Kelsall	$R_{max} = 0.877, R_{fast} = 0.715, k_{fast} = 1.827 \text{ min}^{-1}, k_{slow} = 0.056 \text{ min}^{-1}, R^2 = 0.99846, \text{RMSE} = 0.002$
Pd	
Classic	$R_{max} = 0.771, k = 1.129 \text{ min}^{-1}, R^2 = 0.88364, \text{RMSE} = 1.010$
Klimpel	$R_{max} = 0.801, k = 2.614 \text{ min}^{-1}, R^2 = 0.95269, \text{RMSE} = 0.912$
Second order	$R_{max} = 0.812, k = 2.148 \text{ min}^{-1}, R^2 = 0.97116, \text{RMSE} = 0.859$
Second-order Klimpel	$R_{max} = 0.832, k = 4.592 \text{ min}^{-1}, R^2 = 0.98391, \text{RMSE} = 0.618$
Kelsall	$R_{fast} = 0.673, k_{fast} = 1.520 \text{ min}^{-1}, k_{slow} = 0.017 \text{ min}^{-1}, R^2 = 0.99664, \text{RMSE} = 0.035$
Modified Kelsall	$R_{max} = 0.859, R_{fast} = 0.651, k_{fast} = 1.618 \text{ min}^{-1}, k_{slow} = 0.049 \text{ min}^{-1}, R^2 = 0.99741, \text{RMSE} = 0.011$
2E+Au	
Classic	$R_{max} = 0.771, k = 1.129 \text{ min}^{-1}, R^2 = 0.90524, \text{RMSE} = 0.436$
Klimpel	$R_{max} = 0.801, k = 2.614 \text{ min}^{-1}, R^2 = 0.96364, \text{RMSE} = 0.625$
Second order	$R_{max} = 0.812, k = 2.148 \text{ min}^{-1}, R^2 = 0.97652, \text{RMSE} = 0.646$
Second-order Klimpel	$R_{max} = 0.832, k = 4.592 \text{ min}^{-1}, R^2 = 0.98711, \text{RMSE} = 0.483$
Kelsall	$R_{fast} = 0.673, k_{fast} = 1.520 \text{ min}^{-1}, k_{slow} = 0.017 \text{ min}^{-1}, R^2 = 0.99702, \text{RMSE} = 0.017$
Modified Kelsall	$R_{max} = 0.859, R_{fast} = 0.651, k_{fast} = 1.618 \text{ min}^{-1}, k_{slow} = 0.049 \text{ min}^{-1}, R^2 = 0.99790, \text{RMSE} = 0.005$

Table A6. PGE recovery data fit results of (a) Pt, (b) Pd, and (c) 2E+Au with collector, frother, and depressant concentrations of 30, 30, and 300 g/t, respectively.

Pt	
Classic	$R_{max} = 0.810, k = 1.563 \text{ min}^{-1}, R^2 = 0.92304, \text{RMSE} = 0.104$
Klimpel	$R_{max} = 0.833, k = 4.058 \text{ min}^{-1}, R^2 = 0.96640, \text{RMSE} = 0.487$
Second order	$R_{max} = 0.839, k = 3.560 \text{ min}^{-1}, R^2 = 0.97401, \text{RMSE} = 0.583$
Second-order Klimpel	$R_{max} = 0.853, k = 8.671 \text{ min}^{-1}, R^2 = 0.98363, \text{RMSE} = 0.546$
Kelsall	$R_{fast} = 0.733, k_{fast} = 2.051 \text{ min}^{-1}, k_{slow} = 0.017 \text{ min}^{-1}, R^2 = 0.99641, \text{RMSE} = 0.004$
Modified Kelsall	$R_{max} = 0.870, R_{fast} = 0.704, k_{fast} = 2.293 \text{ min}^{-1}, k_{slow} = 0.066 \text{ min}^{-1}, R^2 = 0.99796, \text{RMSE} = 0.00$
Pd	
Classic	$R_{max} = 0.793, k = 1.232 \text{ min}^{-1}, R^2 = 0.89751, \text{RMSE} = 0.339$
Klimpel	$R_{max} = 0.822, k = 2.895 \text{ min}^{-1}, R^2 = 0.95712, \text{RMSE} = 0.662$
Second order	$R_{max} = 0.833, k = 2.358 \text{ min}^{-1}, R^2 = 0.97028, \text{RMSE} = 0.741$
Second-order Klimpel	$R_{max} = 0.852, k = 6.527 \text{ min}^{-1}, R^2 = 0.98247, \text{RMSE} = 0.623$
Kelsall	$R_{fast} = 0.692, k_{fast} = 1.684 \text{ min}^{-1}, k_{slow} = 0.020 \text{ min}^{-1}, R^2 = 0.99615, \text{RMSE} = 0.012$
Modified Kelsall	$R_{max} = 0.876, R_{fast} = 0.666, k_{fast} = 1.826 \text{ min}^{-1}, k_{slow} = 0.056 \text{ min}^{-1}, R^2 = 0.99730, \text{RMSE} = 0.002$
2E+Au	
Classic	$R_{max} = 0.801, k = 1.374 \text{ min}^{-1}, R^2 = 0.90802, \text{RMSE} = 0.205$
Klimpel	$R_{max} = 0.827, k = 3.355 \text{ min}^{-1}, R^2 = 0.96085, \text{RMSE} = 0.576$
Second order	$R_{max} = 0.836, k = 2.821 \text{ min}^{-1}, R^2 = 0.97148, \text{RMSE} = 0.670$
Second-order Klimpel	$R_{max} = 0.852, k = 6.526 \text{ min}^{-1}, R^2 = 0.98271, \text{RMSE} = 0.593$
Kelsall	$R_{fast} = 0.711, k_{fast} = 1.839 \text{ min}^{-1}, k_{slow} = 0.019 \text{ min}^{-1}, R^2 = 0.99623, \text{RMSE} = 0.007$
Modified Kelsall	$R_{max} = 0.873, R_{fast} = 0.683, k_{fast} = 2.018 \text{ min}^{-1}, k_{slow} = 0.060 \text{ min}^{-1}, R^2 = 0.99758, \text{RMSE} = 0.001$

References

1. Dubiella-Jackowska, A.; Polkowska, Ż.; Namieśnik, J. Platinum group elements in the environment: Emissions and exposure. *Rev. Environ. Contam. Toxicol.* **2008**, *199*, 1–25.
2. Cabri, L.J.; Harris, D.C.; Weiser, T.W. Mineralogy and distribution of platinum-group mineral (PGM) placer deposits of the world. *Explor. Min. Geol.* **1996**, *2*, 73–167.
3. Kettler, P.B. Platinum group metals in catalysis: Fabrication of catalysts and catalyst precursors. *Org. Process Res. Dev.* **2003**, *7*, 342–354. [[CrossRef](#)]
4. Wei, X.; Liu, C.; Cao, H.; Ning, P.; Jin, W.; Yang, Z.; Wang, H.; Sun, Z. Understanding the features of PGMs in spent ternary automobile catalysts for development of cleaner recovery technology. *J. Clean. Prod.* **2019**, *239*, 118031. [[CrossRef](#)]
5. Merker, J.; Lupton, D.; Töpfer, M.; Knake, H. High temperature mechanical properties of the platinum group metals. *Platin. Met. Rev.* **2001**, *45*, 74–82.
6. Zientek, M.L.; Loferski, P.J. *Platinum-Group Elements—So Many Excellent Properties*; US Geological Survey Fact Sheet; US Geological Survey: Reston, VA, USA, 2014; p. 3064.
7. Zientek, M.L.; Loferski, P.J.; Parks, H.L.; Schulte, R.F.; Seal, R.R., II. *Platinum-Group Elements*; N1411339916; US Geological Survey: Reston, VA, USA, 2017.
8. González, J.D.; Yang, Y.; Haynes, B.S.; Montoya, A. Surface coverage effect on ammonia oxidation over Pt (211). *Mol. Catal.* **2023**, *540*, 113048. [[CrossRef](#)]
9. Chen, Q.; Huang, Y.; Hu, X.; Hu, B.; Liu, M.; Bi, J.; Liu, L.; Li, N. A novel ion-solvating polymer electrolyte based on imidazole-containing polymers for alkaline water electrolysis. *J. Membr. Sci.* **2023**, *668*, 121186. [[CrossRef](#)]
10. Golding, T.M.; Omondi, R.O.; Biswas, S.; Chakraborty, S.; Prince, S.; Smith, G.S. Quinolyl-based PGM metallarectangles: Antiproliferative activity, DNA and BSA protein interactions and a molecular docking perspective. *ChemBioChem* **2023**, *24*, e202300271. [[CrossRef](#)]
11. Hughes, A.E.; Haque, N.; Northey, S.A.; Giddey, S. Platinum group metals: A review of resources, production and usage with a focus on catalysts. *Resources* **2021**, *10*, 93. [[CrossRef](#)]
12. Cawthorn, R. The platinum and palladium resources of the Bushveld Complex. *S. Afr. J. Sci.* **1999**, *95*, 481–489.
13. Cawthorn, R.G. Seventy-fifth anniversary of the discovery of the platiniferous Merensky Reef. *Platin. Met. Rev.* **1999**, *43*, 146–148.
14. McDonald, I.; Holwell, D.A.; Armitage, P.E. Geochemistry and mineralogy of the Platreef and “Critical Zone” of the northern lobe of the Bushveld Complex, South Africa: Implications for Bushveld stratigraphy and the development of PGE mineralisation. *Miner. Depos.* **2005**, *40*, 526–549. [[CrossRef](#)]
15. van der Merwe, F.; Viljoen, F.; Knoper, M. The mineralogy and mineral associations of platinum group elements and gold in the Platreef at Zwartfontein, Akanani Project, Northern Bushveld Complex, South Africa. *Mineral. Petrol.* **2012**, *106*, 25–38. [[CrossRef](#)]
16. Holwell, D.; McDonald, I.; Armitage, P. Platinum-group mineral assemblages in the Platreef at the Sandsloot Mine, northern Bushveld Complex, South Africa. *Mineral. Mag.* **2006**, *70*, 83–101. [[CrossRef](#)]
17. Miller, J.; Li, J.; Davidtz, J.; Vos, F. A review of pyrrhotite flotation chemistry in the processing of PGM ores. *Miner. Eng.* **2005**, *18*, 855–865. [[CrossRef](#)]
18. Rule, C. Energy considerations in the current PGM processing flowsheet utilizing new technologies. *J. South. Afr. Inst. Min. Metall.* **2009**, *109*, 39–46.
19. Corin, K.C.; McFadzean, B.J.; Shackleton, N.J.; O’Connor, C.T. Challenges related to the processing of fines in the recovery of platinum group minerals (PGMs). *Minerals* **2021**, *11*, 533. [[CrossRef](#)]
20. Neethling, S.; Cilliers, J. The entrainment of gangue into a flotation froth. *Int. J. Miner. Process.* **2002**, *64*, 123–134. [[CrossRef](#)]
21. Corin, K.; Bezuidenhout, J.; O’Connor, C. The role of dithiophosphate as a co-collector in the flotation of a platinum group mineral ore. *Miner. Eng.* **2012**, *36*, 100–104. [[CrossRef](#)]
22. Taguta, J.; Ross, V. The Application of a Nitrile-based Collector in the Flotation of a Platreef PGM Ore. *Miner. Process. Extr. Metall. Rev.* **2022**, *43*, 716–719. [[CrossRef](#)]
23. Muzenda, E.; Afolabi, A.S.; Abdulkareem, A.S.; Ntuli, F. In Effect of pH on the Recovery and grade of base metal sulphides (PGMs) by flotation. In Proceedings of the World Congress on Engineering and Computer Science, San Francisco, CA, USA, 19–21 October 2011; pp. 19–21.
24. Mokadze, A.M.; Ndlovu, S.; Shemi, A.; Dworzanowski, M. The Reduction of Chrome in UG-2 Flotation Concentrate by Hydrometallurgical Means. *Int. J. Miner. Process. Extr. Metall.* **2021**, *6*, 41–52. [[CrossRef](#)]
25. Uys, N. Flotation of a UG2 Ore in a Novel Pneumo-Mechanical Laboratory Cell. Doctoral Thesis, Stellenbosch University, Stellenbosch, South Africa, 2018.
26. Ralston, O.C. Principles of Flotation. By Ian W. Wark. *J. Phys. Chem.* **1939**, *43*, 816–818. [[CrossRef](#)]
27. Gharai, M.; Venugopal, R. Modeling of flotation process—An overview of different approaches. *Miner. Process. Extr. Metall. Rev.* **2016**, *37*, 120–133. [[CrossRef](#)]
28. Fichera, M.; Chudacek, M. Batch cell flotation models—A review. *Miner. Eng.* **1992**, *5*, 41–55. [[CrossRef](#)]
29. Zuniga, H.G. Flotation recovery is an exponential function of its rate. *Boln. Soc. Nac. Min.* **1935**, *47*, 83–86.
30. Morris, T. Measurement and evaluation of the rate of flotation as a function of particle size. *Trans. Am. Inst. Min. Metall. Pet. Eng.* **1952**, *193*, 794–798.

31. Ramlall, N.; Loveday, B. A comparison of models for the recovery of minerals in a UG2 platinum ore by batch flotation. *J. South. Afr. Inst. Min. Metall.* **2015**, *115*, 221–228. [[CrossRef](#)]
32. McCall, M.-J. Mineralogical and Geochemical Variations in the UG2 Reef at BOOYSENDAL and Zondereinde Mines, with Implications for Beneficiation of PGM. Doctoral Thesis, Stellenbosch University, Stellenbosch, South Africa, 2016.
33. Kelsall, D. Application of probability assessment of flotation systems. *Trans. Inst. Min. Metall.* **1961**, *70*, 191–204.
34. Arbiter, N.; Harris, C. *Froth Flotation*; Fuerstenau, D.W., Ed.; AIME: New York, NY, USA, 1962; p. 215.
35. Mao, L.; Yoon, R.-H. Predicting flotation rates using a rate equation derived from first principles. *Int. J. Miner. Process.* **1997**, *51*, 171–181. [[CrossRef](#)]
36. Hay, M.P.; Roy, R. A case study of optimising UG2 flotation performance. Part 1: Bench, pilot and plant scale factors which influence Cr₂O₃ entrainment in UG2 flotation. *Miner. Eng.* **2010**, *23*, 855–867. [[CrossRef](#)]
37. Cnudde, V.; Boone, M.N. High-resolution X-ray computed tomography in geosciences: A review of the current technology and applications. *Earth-Sci. Rev.* **2013**, *123*, 1–17. [[CrossRef](#)]
38. Godel, B.; Barnes, S.-J.; Maier, W.D. 3-D distribution of sulphide minerals in the Merensky Reef (Bushveld Complex, South Africa) and the JM Reef (Stillwater Complex, USA) and their relationship to microstructures using X-ray computed tomography. *J. Petrol.* **2006**, *47*, 1853–1872. [[CrossRef](#)]
39. Ketcham, R.A.; Carlson, W.D. Acquisition, optimization and interpretation of X-ray computed tomographic imagery: Applications to the geosciences. *Comput. Geosci.* **2001**, *27*, 381–400. [[CrossRef](#)]
40. Nguyen, A.; Schulze, H.J. *Colloidal Science of Flotation*; CRC Press: Boca Raton, FL, USA, 2003; Volume 118.
41. Chen, J.; Chimonyo, W.; Peng, Y. Flotation behaviour in reflux flotation cell—A critical review. *Miner. Eng.* **2022**, *181*, 107519. [[CrossRef](#)]
42. Von Gruenewaldt, G.; Merkle, R. Platinum group element proportions in chromitites of the Bushveld complex: Implications for fractionation and magma mixing models. *J. Afr. Earth Sci.* **1995**, *21*, 615–632. [[CrossRef](#)]
43. Cilek, E. Estimation of flotation kinetic parameters by considering interactions of the operating variables. *Miner. Eng.* **2004**, *17*, 81–85. [[CrossRef](#)]
44. Webb, S.J.; Cawthorn, R.G.; Nguuri, T.; James, D. Gravity modelling of Bushveld Complex connectivity supported by Southern African seismic experiment results. *S. Afr. J. Geol.* **2004**, *107*, 207–218. [[CrossRef](#)]
45. Boudreau, A.E. Modeling the Merensky Reef, Bushveld Complex, Republic of South Africa. *Contrib. Mineral. Petrol.* **2008**, *156*, 431–437. [[CrossRef](#)]
46. Carelse, C.; Manuel, M.; Chetty, D.; Taguta, J.; Safari, M.; Youton, K. The flotation behaviour of liberated Platinum Group minerals in Platreef ore under reduced reagent conditions. *Miner. Eng.* **2022**, *190*, 107913. [[CrossRef](#)]
47. Ramlall, N.V. An Investigation into the Effects of UG2 Ore Variability on Froth Flotation. Doctoral Thesis, University of KwaZulu-Natal, Durban, South Africa, 2013.
48. Corin, K.C.; Wiese, J.G. Investigating froth stability: A comparative study of ionic strength and frother dosage. *Miner. Eng.* **2014**, *66–68*, 130–134. [[CrossRef](#)]
49. Becker, M.; Wiese, J.; Ramonotsi, M. Investigation into the mineralogy and flotation performance of oxidised PGM ore. *Miner. Eng.* **2014**, *65*, 24–32. [[CrossRef](#)]

Disclaimer/Publisher’s Note: The statements, opinions and data contained in all publications are solely those of the individual author(s) and contributor(s) and not of MDPI and/or the editor(s). MDPI and/or the editor(s) disclaim responsibility for any injury to people or property resulting from any ideas, methods, instructions or products referred to in the content.